Supporting Information

Resonance Energy Transfer Approach and A New Ratiometric Probe for Hg^{2+} in Aqueous Media and Living Organism

Moorthy Suresh, Sandhya Mishra, Sanjeev Kumar Mishra, E. Suresh, Amal K. Mandal, Anupama Shrivastav and Amitava Das*

Contents

1. Material and methods:

Reagents used:

Rhodamine 6G, 2-thiophenaldehyde, Hydrazine hydrate, Dansyl chloride were purchased from Sigma-Aldrich (USA). Methanol, Ethanol, Chloroform (AR Grade) and HPLC water were obtained from S.D. Fine Company (India).

Absorption emission and fluorescence decay experiments.

Absorption Spectra were recorded with Varian Cary 500 Scan Uv-vis-NIR Spectrophotometer. While room temperature luminescence spectra and fluorescence decay data were recorded with HORIBA JOBIN YVON spectrophotometer. AXIO IMAGER, Carl Ziess, instrument was used for recording microscopic imaging experiments. OLYMPUS 1 X 81 with FV1000 confocal laser microscope was used for recoding confocal images.

Synthesis of Rhodamine 6G hydrazone (I), compound L_1 and L_2:

Rhodamine 6G hydrazone (I) was prepared following a literature method.[1]

Procedure for the synthesis of L_1:

Rhodamine 6G hydrozide (I; 0.85 mmol, 0.365 g) and thiophene-2-carbaldehyde (1.0 mmol, 0.110 g) were stirred in boiling methanol with 3 drops of acetic acid. After 2 h of

stirring, white precipitates was obtained. This was filtered off, washed with methanol/ether (1:1) mixture and dried over P_2O_5. Yield: 75% (. ^{1}H-NMR (500 MHz, d_6-DMSO), (ppm): 8.762 (1H, s), 7.886-7.871 (1H, d, *J* = 7.5), 7.597-7.528 (3H, m), 7.178-7.172 (1H, d, *J* = 3), 7.004-6.987 (2H, t, J = 4.5), 6.309 (2H, s), 6.155 (2H, s), 5.069-5.049 (2H, s), 3.134-3.095 (4H, q, *J* = 6.5), 1.834 (6H, s), 1.209-1.181 (6H, t, *J* = 7). ^{13}C NMR (500 MHz, d_6-DMSO), (ppm): 164.0, 151.9, 148.2, 142.2, 140.2, 134.3, 131.2, 129.4, 129.1, 128.8, 128.2, 127.2, 124.1, 123.4, 118.7, 105.2, 96.2, 65.9, 37.9, 17.4, 14.6. ESI-MS: m/z = 523.31 for $[L_1+H]^+$, cal. for $C_{31}H_{30}N_4O_2S_1$, L_1, 522.66

Synthesis of L_2:

0.3 g (0.57 mmol) of **L_1** and 80 µl of dry triethyl amine was dissolved in 50 ml dry chloroform under N_2 atmosphere. To this solution 0.158 g (0.58 mmol) of dansyl chloride was added and refluxed for 24 hours. The organic layer was washed 3 times with 50 ml of water and dried over anhydrous Na_2SO_4. Finally the crude was purified by column chromatography using $CHCl_3$/MeOH (99:1) as an eluent to give 0.135 g of organge color solid of **L_2** of 30% yield. ^{1}H-NMR (500 MHz, $CDCl_3$), (ppm): 8.644 (1H, s), 8.009-7.992 (1H, d, *J* = 8.5), 7.479-7.465 (4H, m), 7.227-7.218 (2H, d, *J* = 4.5), 7.068-7.051 (2H, d, *J* = 8.5), 7.018-7.011 (2H, d, J = 3.5), 6.887-6.879 (2H, t, *J* = 4.5), 6.400 (2H, s), 6.329 (2H, s), 3.480 (2H, s), 3.201 (6H, s), 1.873 (6H, s), 1.667 (2H, s), 1.327-1.298 (6H, t, *J* = 7.5). ^{13}C NMR (500 MHz, $CDCl_3$), (ppm): 164.8, 151.9, 151.4, 147.5, 141.2, 141.0, 133.3, 129.5, 129.3, 128.9, 128.2, 127.8, 127.7, 126.9, 123.7, 123.3, 122.8, 118.3, 117.9, 116.0, 106.2, 96.7, 66.0, 45.4, 38.3, 29.7, 16.7, 14.7. ESI-MS: m/z = 794.32 for $[\mathbf{L_2}+K]^+$, cal. for $C_{43}H_{41}N_5O_4S_2$, L_2, 755.95.

(1). Wu, D.; Huang, W.; Duan, C.; Lin, Z.; Meng, Q. *Inorg. Chem*. **2007**, *46*, 1538-1540.

2. ^{1}HNMR Spectrum of L_1:

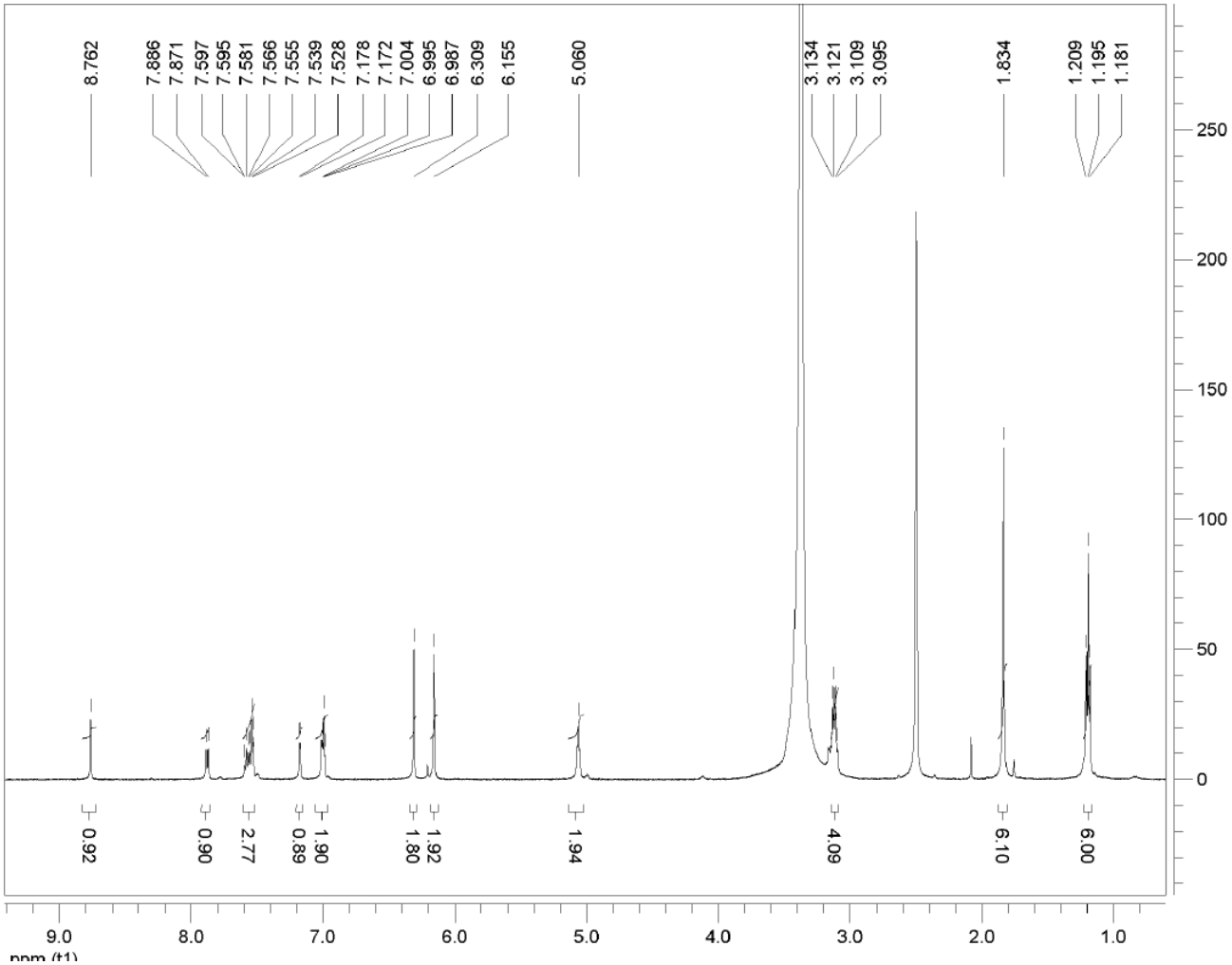

SI Figure 1: ^{1}H NMR spectra recorded for **L_1** in d_6 DMSO**.**

3. ^{13}C NMR Spectrum of L_1:

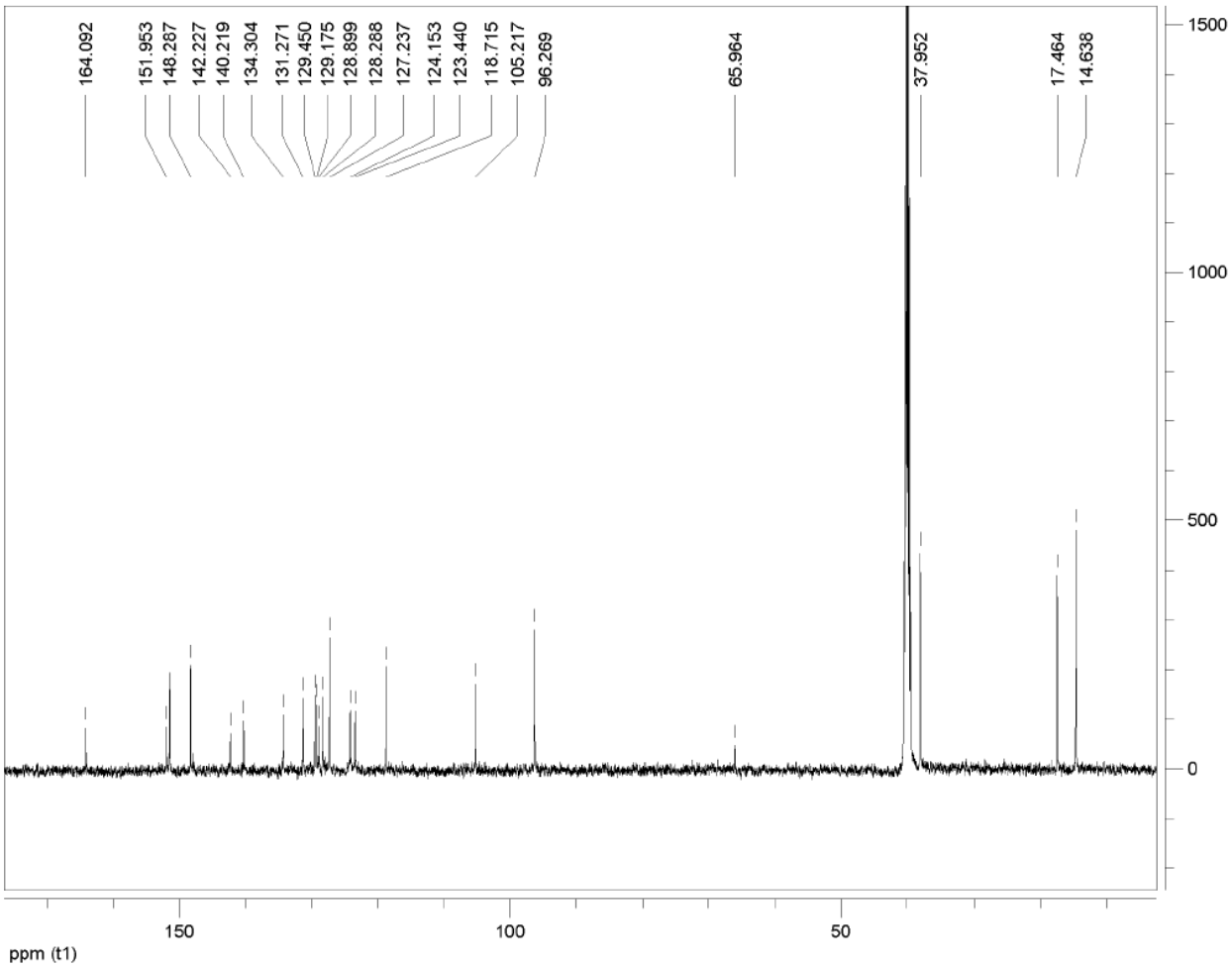

SI Figure 2: ^{13}C NMR spectra recorded for **L_1** in d_6 DMSO

4. Mass Spectrum of L_1:

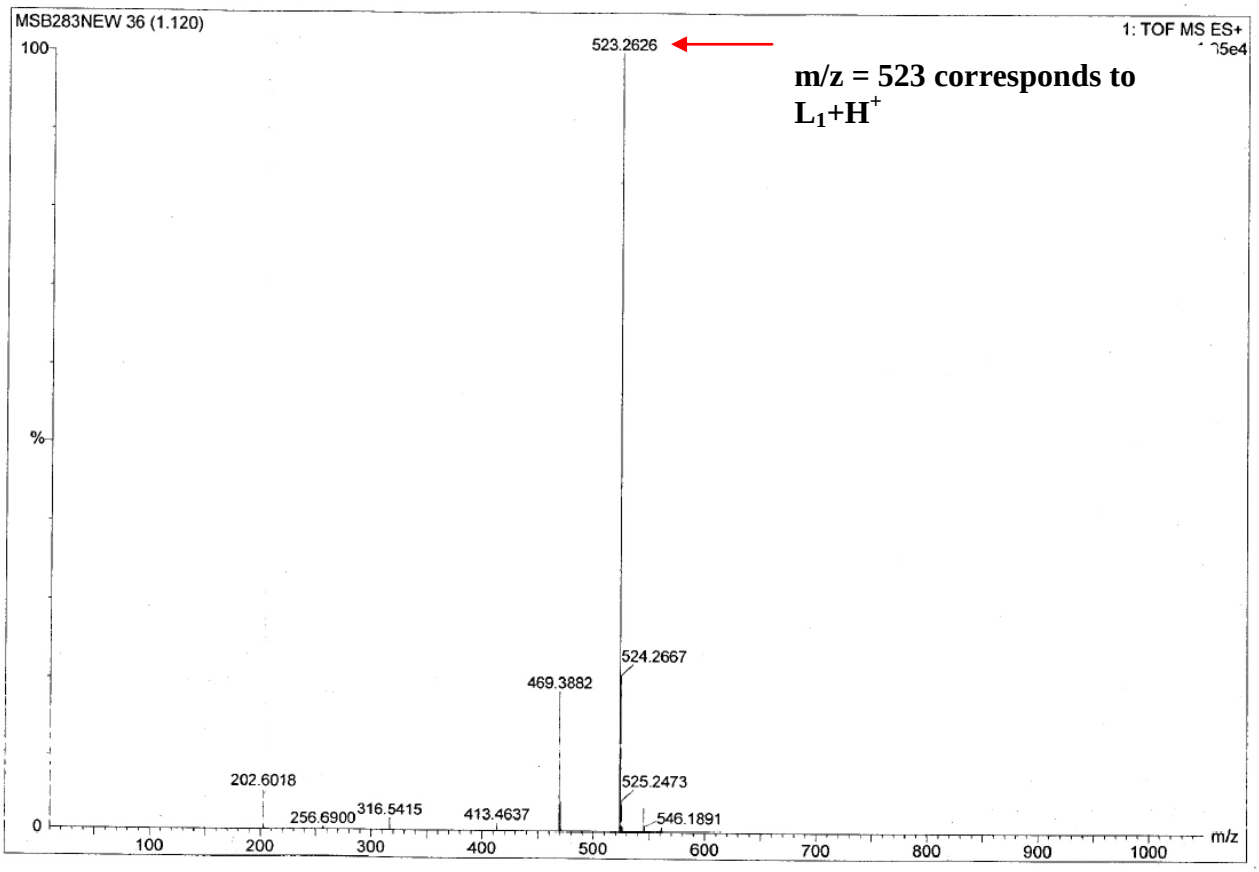

SI Figure 3: ESI-Ms spectra for **L_1**.

5. NMR spectrum of L_2

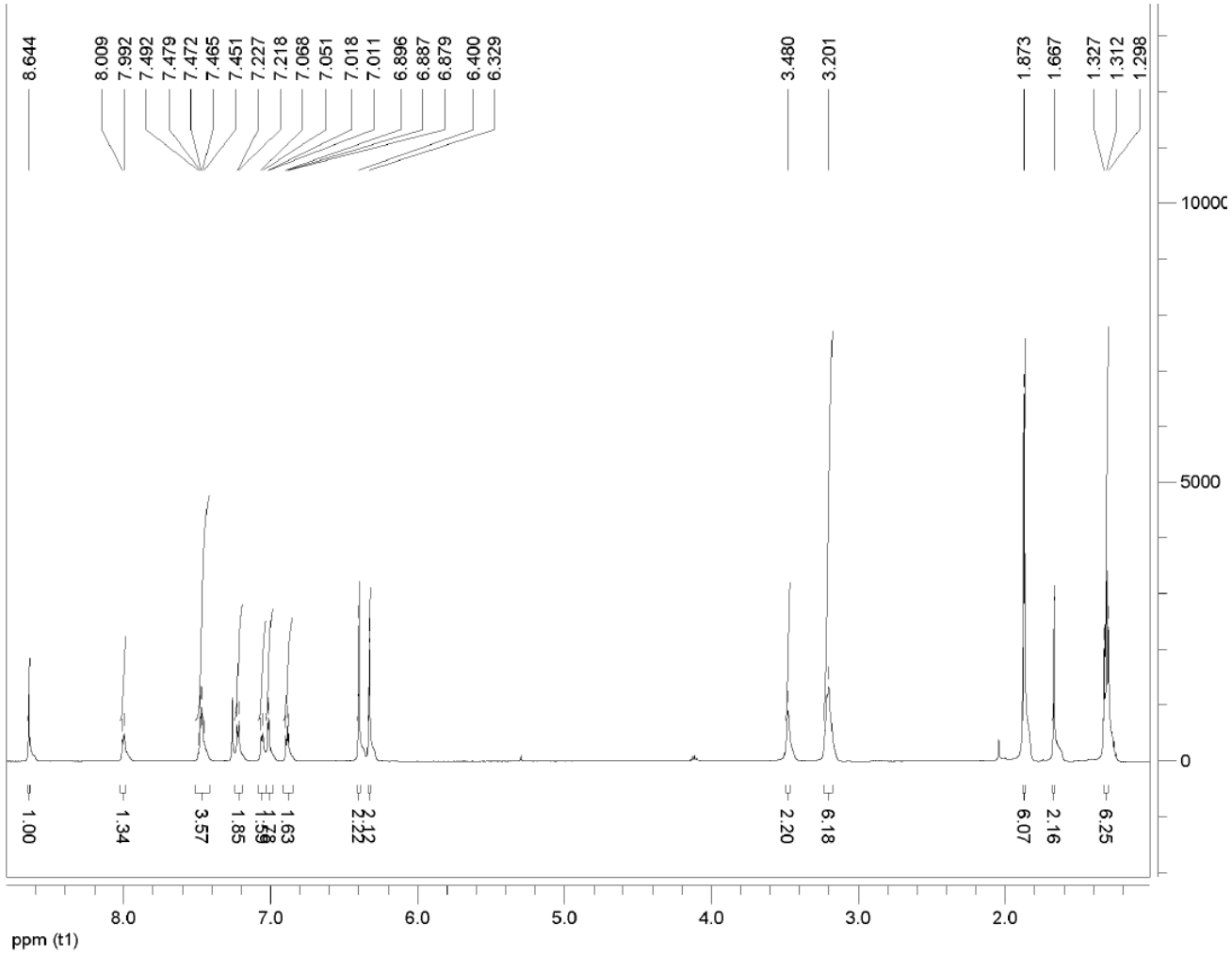

SI Figure 4: ^{1}H NMR spectra recorded for **L_2** in $CDCl_3$**.**

6. ^{13}C NMR spectrum of L_2

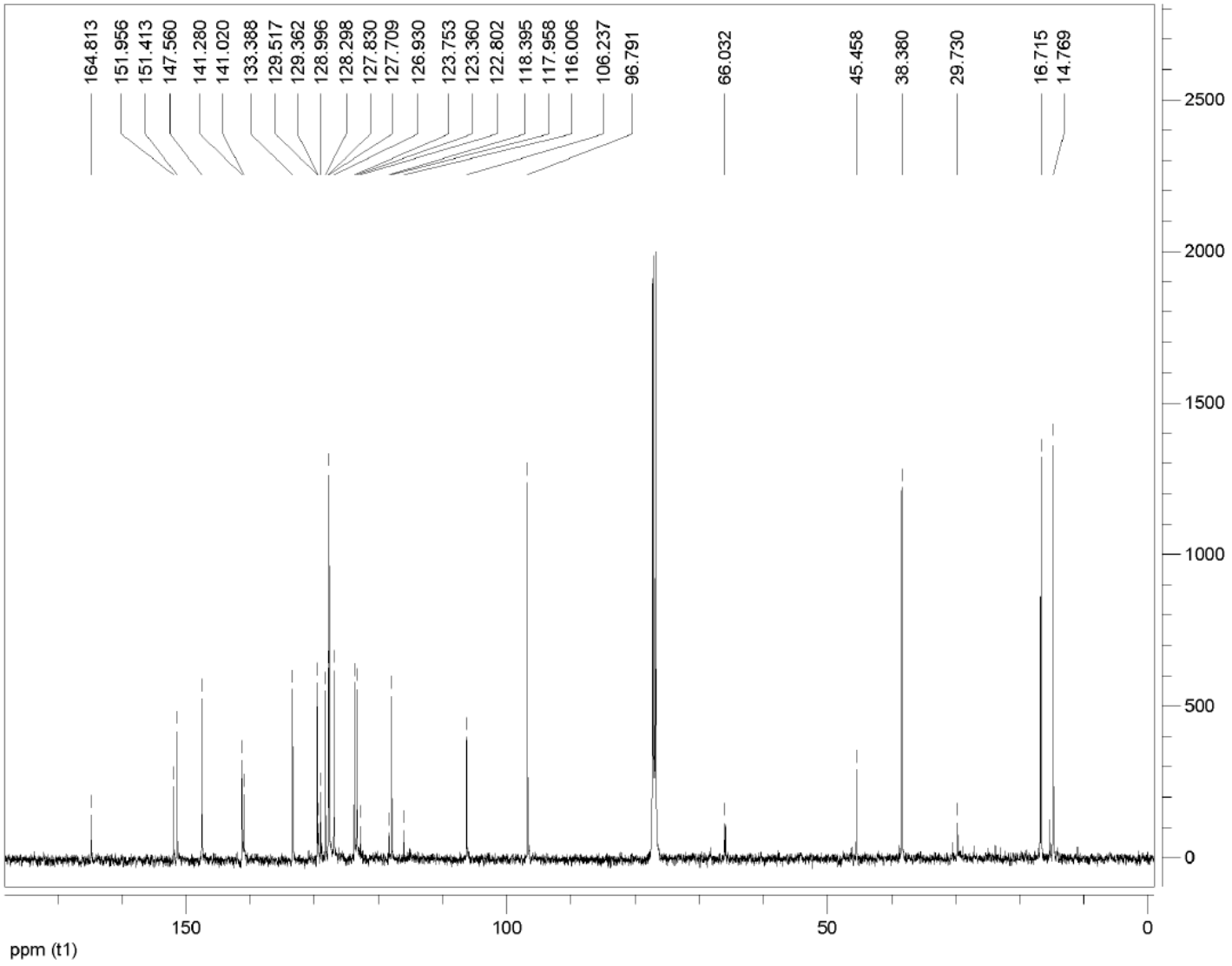

SI Figure 5: ^{13}C NMR spectra recorded for **L_2** in $CDCl_3$**.**

7. Crystal structure of L_1:

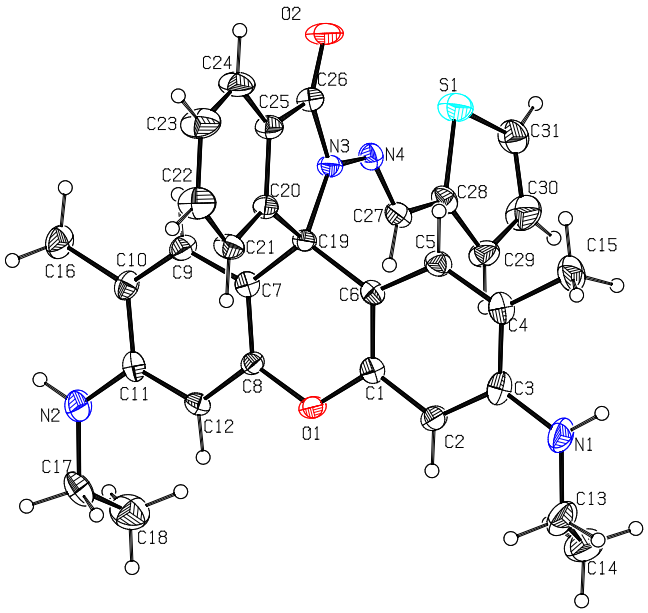

SI Figure 6: ORTEP diagram of the compound L_1 (30% probability factor for the thermal ellipsoids)

8. Mass spectrum of L_2:

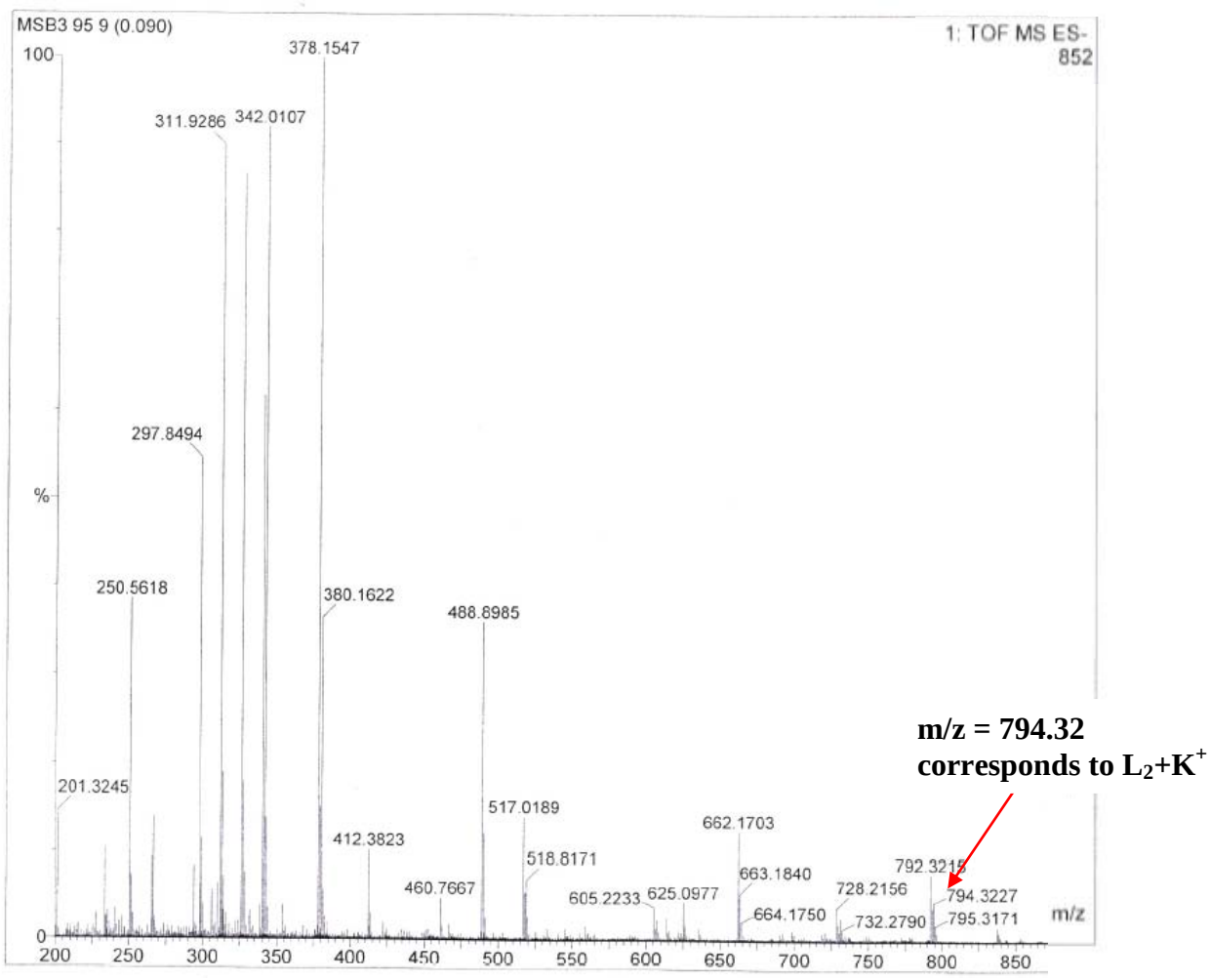

SI Figure 7: ESI-Ms spectra for **L_2**.

9. Changes in the Absorption spectra with various other metal ions:

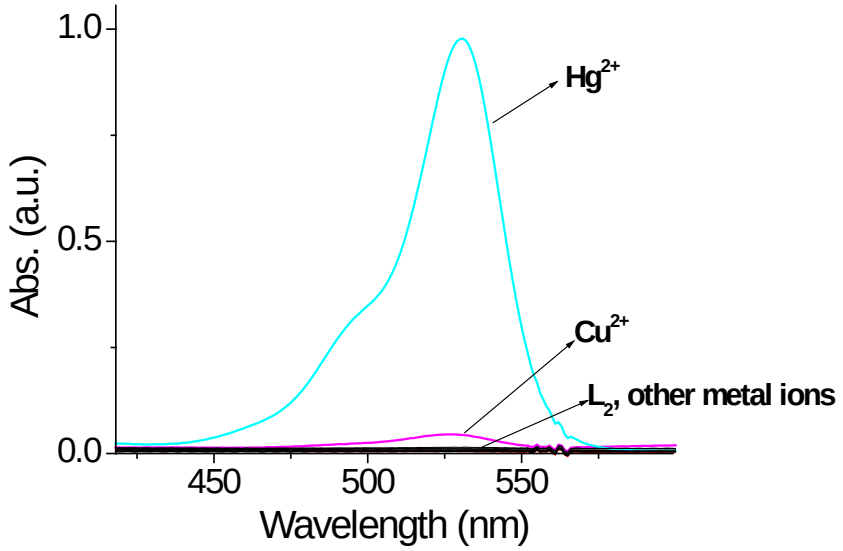

SI Figure 8: Changes in the absorption spectra of $\mathbf{L_1}$ (5.0×10^{-5}M) in the presence of various other metal ions (Co^{2+}, Ni^{2+}, Cu^{2+}, Ca^{2+}, Cd^{2+}, Co^{2+}, Mg^{2+}, Zn^{2+}, Hg^{2+}, Na^{+}, K^{+}, Fe^{2+}) (5.0×10^{-4} M) in water/acetonitrile (1:1, v/v) mixture.

10. Absorption based competitive metal ions study with Hg^{2+}

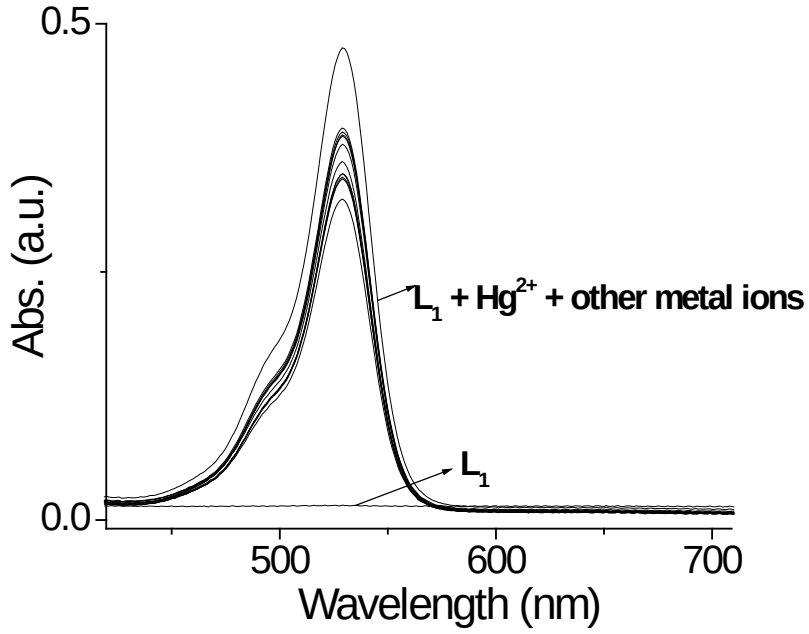

SI Figure 9 : Change in the absorption spectra of $\mathbf{L_1}$ (6.0×10^{-5}M) in the presence of Hg^{2+} (2.0×10^{-4}M) with various other metal ions (Co^{2+}, Ni^{2+}, Cu^{2+}, Ca^{2+}, Cd^{2+}, Co^{2+}, Mg^{2+}, Zn^{2+}, Na^{+}, K^{+}, Fe^{2+}) (2.0×10^{-4}M) in water/acetonitrile (1:1, v/v) mixture.

11. Fluorescence scanning with different metal ions:

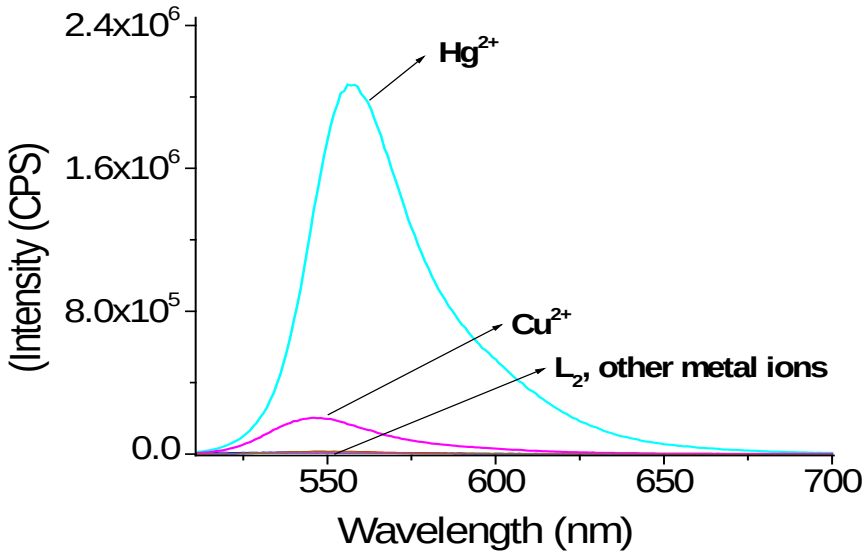

SI Figure 10: Change in the emission spectra of $\mathbf{L_1}$ (5.0 x 10^{-5}M) in the presence of various metal ions (Hg^{2+}, Co^{2+}, Ni^{2+}, Cu^{2+}, Ca^{2+}, Cd^{2+}, Co^{2+}, Mg^{2+}, Zn^{2+}, Na^{+}, K^{+}, Fe^{2+}) (5.0 x 10^{-4}M) in water/acetonitrile (1:1, v/v) mixture. λ_{ext}: 500 nm.

12. UV Titration with Copper perchlorate:

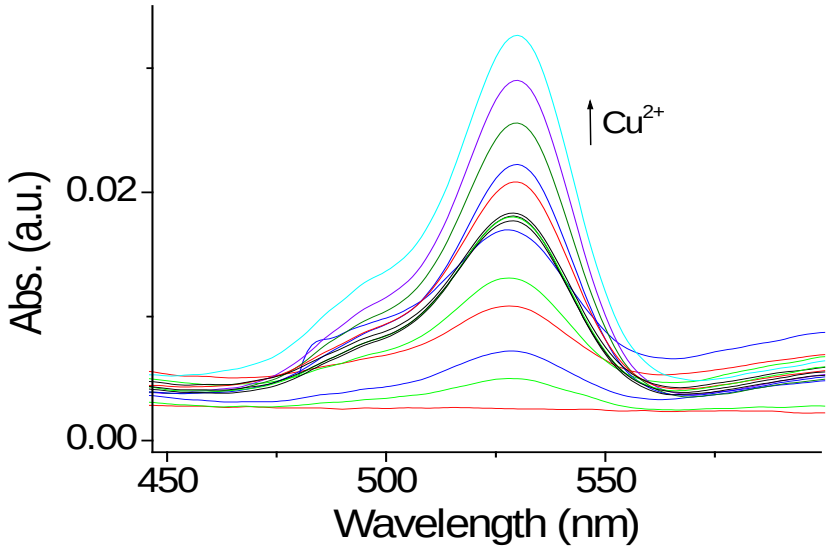

SI Figure 11: Change in the absorption spectra of $\mathbf{L_1}$ (2.0×10^{-5}M) upon addition of varying [Cu^{2+}] of ($0 - 8.0 \times 10^{-4}$M) Cu^{2+} in water/acetonitrile (1:1, v/v) mixture.

13. Fluorescence titration with copper perchlorate:

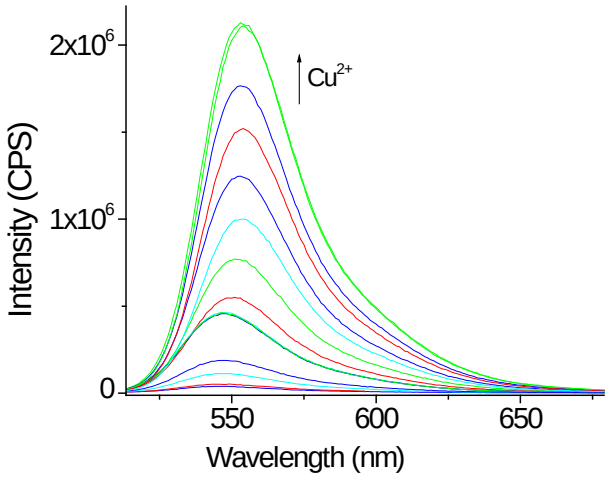

SI Figure 12: Change in the fluorescence spectra of $\mathbf{L_1}$ (2.0×10^{-5}M) upon addition of varying [Cu^{2+}] (0 - 8.0×10^{-4}M) Cu^{2+} in water/acetonitrile (1:1, v/v) mixture [λ_{ext} = 500 nm].

14. Changes in the Absorption spectra of L_2 with various other metal ions:

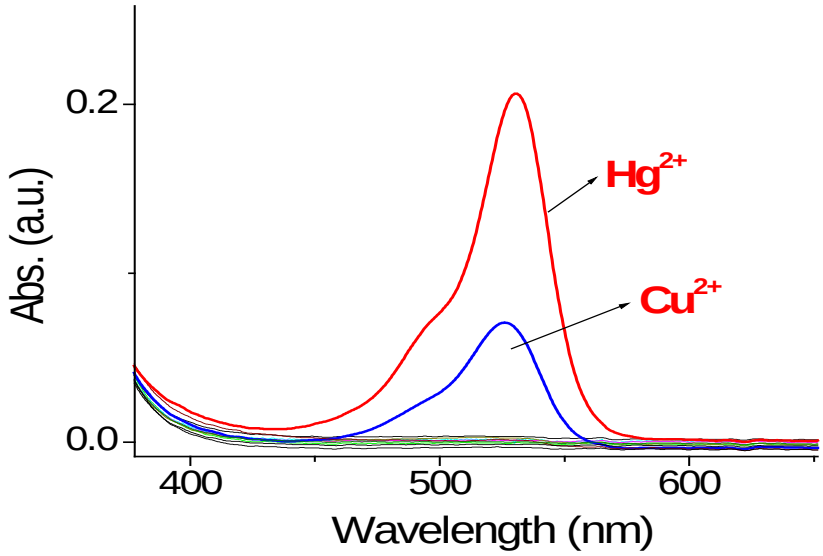

SI Figure 13: Changes in the absorption spectra of $\mathbf{L_2}$ (5.0×10^{-5}M) in the presence of various other metal ions (Co^{2+}, Ni^{2+}, Cu^{2+}, Ca^{2+}, Cd^{2+}, Co^{2+}, Mg^{2+}, Zn^{2+}, Hg^{2+}, Na^{+}, K^{+}, Fe^{2+}) (5.0×10^{-4} M) in water/acetonitrile (1:1, v/v) mixture.

15. Fluorescence scanning study for L_2:

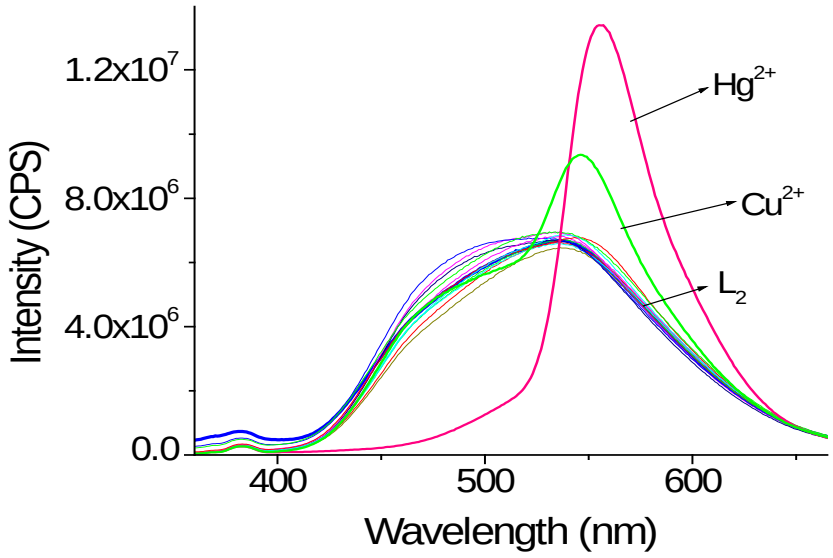

SI Figure 14: Changes in the emission spectra of **L_2** (1.0×10^{-5}M) in the presence of various other metal ions (Co^{2+}, Ni^{2+}, Cu^{2+}, Ca^{2+}, Cd^{2+}, Co^{2+}, Mg^{2+}, Zn^{2+}, Hg^{2+}, Na^{+}, K^{+}, Fe^{2+}) (4.0×10^{-4} M) in water/acetonitrile (1:1, v/v) mixture.

16. Job's plot

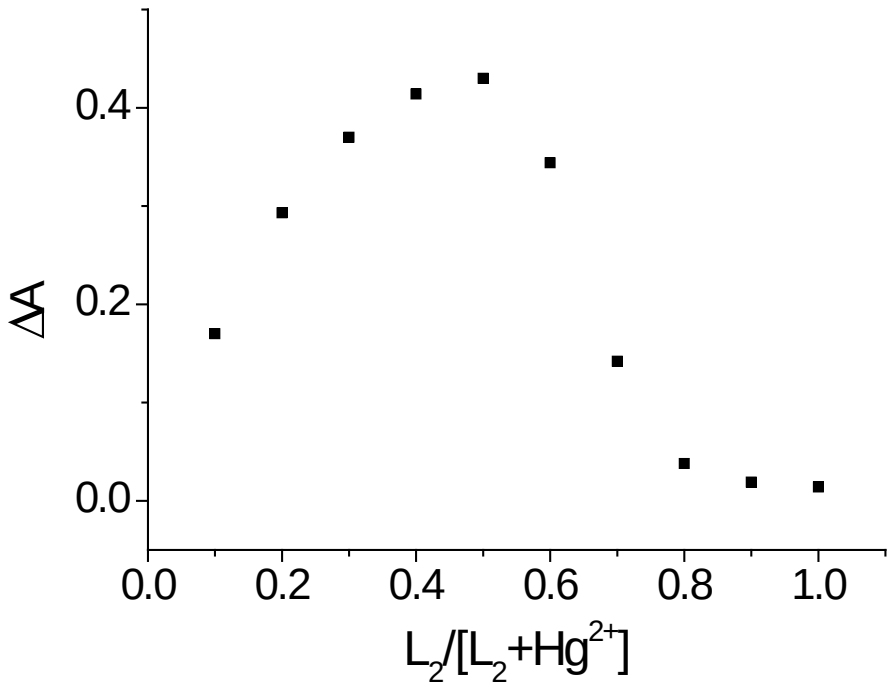

SI Figure 15: Job's plot of the complexation between L_2 and Hg^{2+}. Total concentration of $[L_2]+[Hg^{2+}] = 2.0 \times 10^{-4}$M

17. Reversible binding study with EDTA:

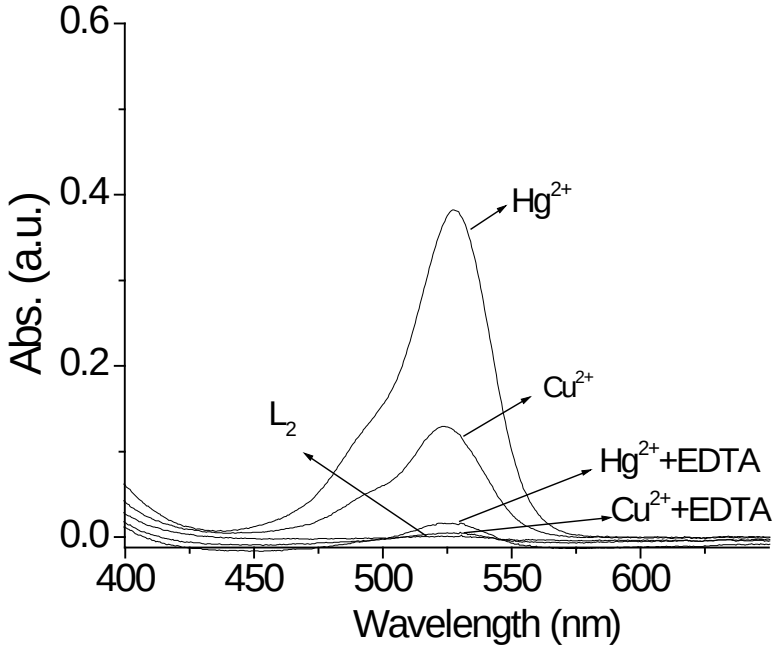

SI Figure 16: Uv-vis spectra of $\mathbf{L_2}$ (5.0×10^{-5}M) in the presence of 10 mole equivalents of Hg^{2+} and Cu^{2+}. Excess of EDTA was added to $\mathbf{L_2}$+M^{2+} in water/acetonitrile (1:1, v/v) mixture to show the reversible binding nature of Hg^{2+}/Cu^{2+} with $\mathbf{L_2}$

18. Absorption spectra of L_1 and L_2

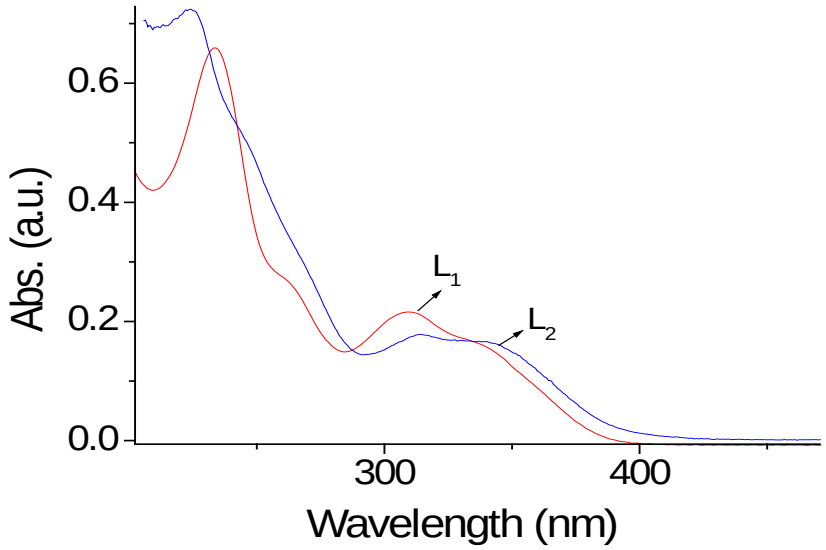

SI Figure 17: Absorption spectra of **L_1** and **L_2** (5.0×10^{-5}M) in water/acetonitrile (1:1, v/v) mixture.

19. Visible and fluorescence color changes:

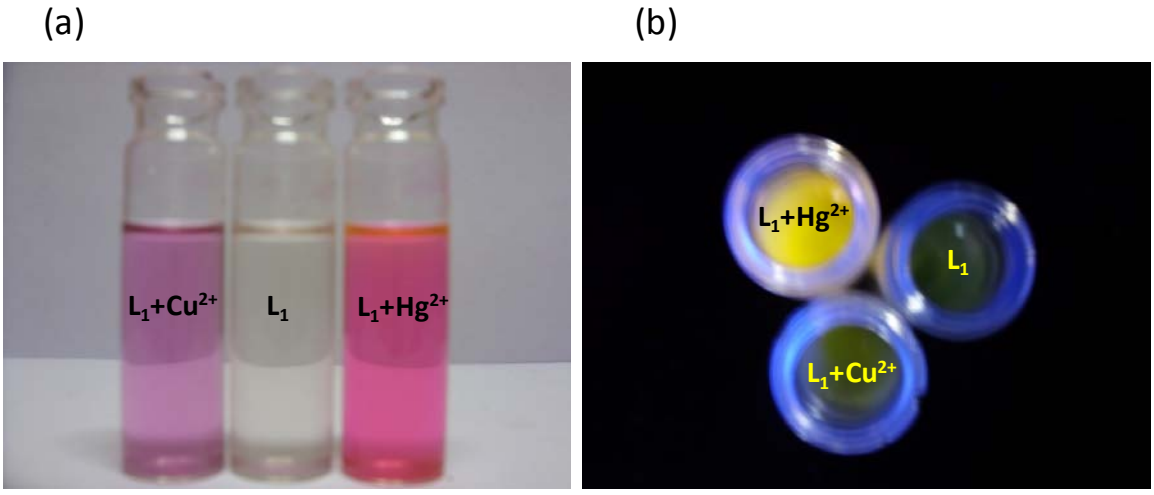

SI Figure 18: Visible (a) and fluorescence (b) color change of **L_1** (10×10^{-6} M) in the presence of 10 mole equivalents of Hg^{2+} and Cu^{2+} in water/acetonitrile (1:1, v/v) mixture.

20. Bacterial cell growth:

Pseudomonas putida was cultured in the King's B (KB) medium (Peptone 20g, glycerol 15g, K_2HPO_4 1.5 g, $MgSO_4.7H_2O$ 1.5 g, distilled water 1000 ml, pH 7.2). The cells were harvested and vortexed for making the homogenous suspension in sterile distilled water. The cultured cells were first exposed to different concentration of Hg^{2+} for 10 min at 25°C in 1:1 ethanol/water mixture. After 10 min, the unabsorbed Hg^{2+} was removed through centrifugation in order to avoid the background fluorescence while recording fluorescence microscope images. The centrifuged bacterial cells were finally exposed to $\mathbf{L_2}$ under the same condition and confocal images were recorded.

21. FRET calculation:

The forster distance R_0 can be calculated by

$$R_0 = 9.79 \times 10^3 [(J)\, Q\, (n^{-4})\, (\kappa^2)]^{1/6}$$

Where n is the refractive index of the medium in between donor and acceptor and was taken approximately to be equal to 1.4. $\square^2$ is the dipole orientation factor. Depending upon the relative orientation of donor and acceptor, the value ranges from 0 - 4 and it is often assumed to be 2/3. Q is the fluorescence quantum yield of the donor in the absence of acceptor.
J is the spectral overlap integral between the emission spectrum of the donor and the absorption spectrum of the acceptor and was given by the following expression

$$J = \int f_D(\lambda)\, \varepsilon(\lambda)\, \lambda^4\, d\lambda$$

$f_D(\lambda)$ is the normalised emission of the donor. $\varepsilon(\lambda)$ is the molar absorption coefficient ($M^{-1}\, Cm^{-1}$) of the donor.

22. Equations:

Equation 1: Energy transfer efficiency (Φ_{ET}).

$\Phi_{ET} = 1-(F'_D/F_D)$ Eq. 1

F'_D and F_D denote the donor fluorescence intensity with and without an acceptor, respectively

Equation 2: Energy transfer rate constant (k_{ET}).

τ_D denotes the fluorescence lifetime of the donor fragment in the absence of acceptor.